Peripheral Nerve Conduction Block with High Frequency Stimulation via Percutaneous Lead Electrode

A THESIS
SUBMITTED TO THE FACULTY OF THE GRADUATE SCHOOL
OF THE UNIVERSITY OF MINNESOTA
BY

Xuan Wei

IN PARTIAL FULFILLMENT OF THE REQUIREMENTS
FOR THE DEGREE OF
MASTER OF INTEGRATED BIOLOGY AND PHYSIOLOGY

John W. Osborn

May 2011

© Xuan Wei 2011

Acknowledgements

"Appreciation is a wonderful thing.

It makes what is excellent in others belong to us as well."

– Voltaire

While some say it is easy to blame our parents for everything that is wrong with us and our lives, it is even easier to credit them for every progress we make. My parents, Zhijun Wei and Aixian Liang, have taught me both the value of formal education and the desire to be a life-long learner. If nothing else, these two values enrich and benefit me everyday. I am eternally grateful to them.

My advisor, Dr. John W. Osborn, Jr., embodies the rare brilliance of having all the wisdom to tell others what to do, but instead helping them find out the answers themselves. If you have been as lucky as I am, you know how wonderful this is. His abundance and generosity make him the last professor you want to disappoint. Just ask his tireless students who run experiments in the lab around the clock, happily.

I want to thank my committee members Dr. Stephen A. Katz and Dr. William C. Engeland. Dr. Katz has a perfect balance of meticulous quality control and steady reason. He is always there to provide guidance on things that I may have missed otherwise. I know that if Dr. Katz says I am OK, then I am OK. It has been a delight working with Dr.

William C. Engeland. Professor Engeland has been very responsive to my requests and always provided great advice.

Dr. Nico J. M. Rijkhoff at Aalborg University, Denmark has been instrumental in helping me establish animal model and experiment procedures used in various projects over the years. This study is no exception. Known as a leading researcher in the field of electrical stimulation and neuroprosthesis, Dr. Rijkhoff has a no-nonsense rigorous approach to research. At the same time, he is down-to-earth, open to share, passionate to teach, and fun to work with. I feel very fortunate be able to consider Dr. Rijkhoff as a key mentor of mine.

My daughter Kira Rayne Hasse, in addition to bringing me endless joy of being a new mother, also helped me to gain more clarity in my priorities and be more efficient with my time. Thank her for being a happy and self-sufficient baby most of the time!

But the real person who made it all easy for me was Ryan Hasse, my best friend and partner in crime for life. I know I can always count on Ryan for love and care, for private jokes and heartfelt laughter, for kindness and enlightenment, for being the best daddy Kira could possibly have, and for all the good years to come supporting each other.

This work would have not been possible without the support from Medtronic Neuromodulation and the people who make it great. Mark Lent has not only taught me

critical thinking based on first principals, a quality that is essential in assessing technologies for medical therapies, but also provided abundant opportunities for me to exercise it. Dr. Timothy Denison provided inspiration for many, including myself, at Medtronic with his ingenuity and passion and for world-class medical technologies. To me, Keith Miesel represents vision, competency, humility, kindness, and support one can count on. Eric Panken always provided candid insights and wisdom when one needed it. It was through a class of neuroscience at the University of Minnesota Medical School where we all first met, and where my journey with Medtronic began.

I would also like to thank William Schindeldecker, Dr. Luis Ramon, and Dr. Matthew Kelly at Medtronic Physiological Research Laboratories. They helped to ensure that animals were treated in the most humane way possible, and that the experiments were conducted according to the highest standards toward the goal of creating emerging medical therapies to benefit the human kind. That's the magic of Medtronic, a company that for 60 years has stayed focused on its mission: "To contribute to human welfare by application of biomedical engineering in the research, design, manufacture, and sale of instruments or appliances that alleviate pain, restore health, and extend life."

Dedication

This thesis is dedicated to individuals who suffer from chronic neurological disorders.

Abstract

Nerve conduction block elicited by high frequency electrical stimulation may be used to create chronic neuroprostheses to treat diseases that are characterized by pathological nervous activities. Previous studies have demonstrated that local and reversible nerve conduction block can be achieved using high frequency stimulation (3-6 kHz and above) delivered through cuff electrodes. However, cuff electrodes are designed to be placed encircling the nerve and demands invasive surgical procedure that may not be desired by patients in clinical applications. This study investigated the nerve block effect of high frequency stimulation delivered through a percutaneous lead placed next a motor nerve trunk in dogs. The optimal frequency and amplitude windows for nerve block using a biphasic rectangular waveform were 10-30 kHz and 15-20 V peak-to-peak within the tested parameter range (5-40 kHz and 5-20 V). Higher frequencies may require higher amplitudes to achieve nerve block effect. In addition, activation threshold of the nerve evoked by the biphasic high frequency stimulation also increased with frequency. The HFS nerve block was repeatable in more than 40 minutes of repetitive stimulation. This study demonstrated that it is feasible to achieve local reversible nerve block using percutaneous lead electrodes placed next to a nerve with biphasic high frequency waveform. Although it may be difficult to block all the nerve fibers in a nerve trunk with a percutaneous lead, partial nerve block can be clinically useful and desired in many disease conditions.

Table of Contents

List of Tables

List of Figures

List of Abbreviations

AC	Alternating current
BR	Block ratio
BE	Block efficiency
CAP	Compound action potential
DBS	Deep Brain Stimulation
DC	Direct current
DS	Distal stimulation
EUS	External urethral sphincter
HFS	High frequency stimulation
HH	Hodgkin-Huxley (model)
LFS	Low frequency stimulation
MRG	McIntyre, Richardson, and Grill (model)
RR	Reversibility ratio

Units:

ºC	degree Centigrade
Fr	French gauge (0.33mm)
Hz	hertz
kHz	kilohertz

mA	milliamper
mm	millimeter
ms	millisecond
μC	microcoulomb
μm	micron (micrometer)
V	volt

1 Introduction

1.1 Clinical motivation

In the past two decades, neuromodulation systems have achieved great clinical success in treating patients with various disorders including chronic pain, overactive bladder and urinary retention, Parkinson's disease, essential tremor, and dystonia[1-3]. While most existing clinical neuromodulation systems elicit *activation* of the target nervous tissue to "modulate" the nervous system, creating *conduction block* of the target nerves may provide additional therapeutically opportunities to restore function by reducing or eliminating pathological signals in the nervous system.

Nerve conduction block may be used to treat diseases that are characterized by pathological afferent activities, such as chronic pelvic pain, interstitial cystitis, abacterial chronic prostatitis (Type IIIB), neuromas, neuralgias, and other chronic pain conditions, as well as diseases with pathological motor activities, such as spasticity, pelvic floor disorders, tics, chorea, and intractable hiccups. Abnormal afferent and efferent hyperactivities may cause pain, overwhelm central processing, inhibit associated neural activities through reflex pathways, and cause permanent musculoskeletal deformities or contractures[4]. Nerve conduction block may reduce pathological hyperactivities and restore normal function. Nerve conduction block can also be used in combination with nerve stimulation to provide selective activation of certain nerve fibers and signal propagation in a certain direction and generate a normal pattern of neural signals to restore function.

1.2 Nerve conduction block techniques

1.2.1 Definition of nerve conduction block

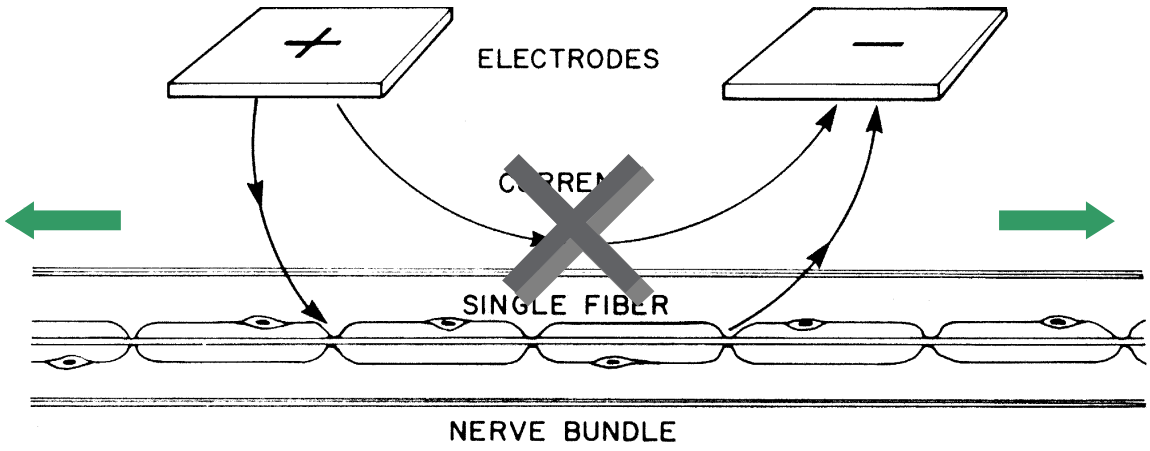

Figure 1: An illustration of the ideal nerve block effect

For the purpose creating chronic neuroprostheses to restore function, nerve conduction block is defined as preventing propagation of action potentials across the site of stimulation, as illustrated in Figure 1. An ideal nerve block effect is local, reversible, and repeatable. The block effect should be local, such that the action potentials can still propagate away from the block site. For instance, excitations proximal to the nerve block site can propagate afferently and excitations distal to the nerve block site can propagate efferently. The nerve block should be reversible, such that the nerve and its innervated tissues should be responsive to excitations shortly after the cessation of the nerve block stimulation. Specifically, when nerve block is applied to a motor nerve, there should be minimum fatigue of the neuromuscular junction associated with the nerve, such that the musculature can respond to nerve stimulation distal to the nerve block site during the

block period, and can respond to stimulation proximal to the nerve block site shortly after the block period. Finally, the nerve block should be repeatable, such that the chronic neuroprosthesis can achieve effective block effect with repetitive deployment over a long period of time.

1.2.2 Overview of existing nerve conduction block techniques

Many non-electrical techniques exist for nerve conduction block. These include pressure application[5-6], local temperature manipulation[7-8], and surgical and pharmacological methods[4, 9-13]. However these methods are non-specific, have poor or slow reversibility, and may cause potential nerve damage and side effects. Therefore they are not suitable for chronic neuroprosthetic applications.

Suppression of axonal conduction using electrical stimulation has been a topic of interest for many decades[14-15]. Hypothesized axonal suppression effects through electrical stimulation may include the influence of the axonal refractory period on evoked excitation, desynchronization of the underlying units of the compound action potential (CAP), an increase in the threshold for evoked excitation, and sodium or potassium mediated depolarization blockade[16-21]. The exact mechanisms of the electrical stimulation techniques are usually unclear and controversial.

It has been demonstrated that direct current (DC) can induce conduction block of nerve fibers[22-23]. However, DC nerve block is not a practical tool for chronic neuroprostheses, because DC nerve block can damage the nerve due to electrode polarization[24].

Collision block is a technique that elicits nerve block by intercepting orthodromic nerve impulses with evoked antidromic nerve impulses[25-26]. This technique typically uses quasi-trapezoidal stimulation and tripolar cuff electrodes with a cathode flanked by two anodes. By distributing current unequally between the anodes or placing one anode nearer to cathode than the other, action potentials can be allowed to escape unidirectionally during stimulation[26]. There is a window of effective stimulation amplitudes that are needed for unidirectional stimulation, below which the anodal block is not effective and above which virtual cathodes can be generated to cause stimulation. The collision block technique may require cuff electrodes to be placed encircling the nerve, which is a more invasive surgical procedure than what is required to implant percutaneous lead electrodes in most clinical applications.

Some research has shown that for Deep Brain Stimulation (DBS), frequencies of 50-300 Hz may be used to suppress somatic and axonal activities in the brain[16, 27-28]. It was suggested that the mechanism of this suppression may be depolarization blockade mediated by elevations in extracellular potassium[16-17]. However, other research has suggested that the above frequency range suppresses somatic activity but activates the axons in the brain[29-33] and replaced the pathological rhythms with regularized firing activity[34-37]. The mechanism of action of DBS is still controversial. It is likely that the mechanism involved in the brain activity suppression in the DBS field differs from the conduction block observed in peripheral nerves where the frequency range is generally in the kilohertz range.

Nerve block of peripheral nerves elicited by high frequency stimulation (HFS) of above 1 kHz has been demonstrated in a number of animal models. The optimal frequencies for a nerve block effect were typically in the range of 3-30 kHz [21, 38-44]. Nerve block achieved in this high-frequency range has been demonstrated to be local and quickly reversible (less than one second), verified by muscle response to excitation distal but not proximal to the block site[21]. For frequencies below 1 kHz, it is possible to observe depressed response to nerve excitation through a fatigue mechanism[45-46], evidenced by lack of reversibility of nerve response tens of seconds to minutes after the cessation of the stimulation[21, 43, 45]. The lack of reversibility may be caused by muscle fatigue, depletion of the neuromuscular junction transmitter, or a mechanism called "neural conduction fatigue", of which the physiological basis is still undetermined[21, 45, 47-49]. In addition, some modeling work suggested that true nerve block can be achieved with frequencies above 2 kHz[50], while other models suggested that true nerve block can only be achieved with frequencies above 5-6 kHz, where below 5-6 kHz the stimulation would lead to a reduction in muscle force caused by depletion of transmitter at the neuromuscular junction[19, 44].

1.3 Nerve Conduction Block Using HFS

1.3.1 HFS waveforms and parameters

For our purpose, we are interested in HFS conduction block for peripheral nerves. Using cuff electrodes and intrafascicular electrodes, animal studies have shown that the amplitude required for nerve block increased with the stimulation frequency[21, 38-41, 44, 51].

This is consistent with modeling results[44, 50]. In addition, the required block amplitude also increased with decreasing nerve fiber diameter[44, 50, 52-53]. Among studies that used cuff electrodes to deliver HFS, there were disparate results of the optimal frequencies (anywhere from 3 kHz to 30 kHz) for nerve conduction block, due to differences among experimental conditions, animal species, and stimulation waveforms. Nevertheless, in general a complete block can be achieved using a cuff electrode with frequencies of 3-6 kHz and above, and amplitudes of 0.6-2 mA and above for current controlled waveforms[21, 38-40] and 1-3 V and above for voltage controlled waveforms[38, 41]. Using intrafascicular electrodes, one study investigated frequencies of 20-40 kHz and achieved complete nerve block with amplitudes of 1.5-6.5 mA[51]. The maximum frequency for HFS block has not been evaluated experimentally, mostly due to equipment limitations.

Using a frog sciatic nerve preparation, one study compared various biphasic HFS waveforms (constant voltage against constant current, and rectangular against sinusoidal) in a frequency range of 600 Hz -20 kHz[21]. It was found that the electrode-tissue impedance appeared to act like a pure resistance at the frequencies tested, and therefore the waveform delivered to the tissue was very similar between current-controlled and voltage-controlled waveforms. In addition, there was no appreciable difference in the characteristics of the responses between the rectangular and sinusoidal waveforms. The waveforms produced blocks at the same amplitudes and frequencies on a charge-per-phase basis. In another study three biphasic HFS waveforms were compared against each other in a cat pudendal nerve preparation: rectangular with pulse width dependent on

frequency (with no pause between cycles), rectangular with pulse width independent of frequency (with a pause between cycles), and sinusoidal, as illustrated in Figure 2[40]. It was found that rectangular waveform with pulse width dependent on frequency was more effective for blocking motor pathways than rectangular waveform with pulse width independent of frequency and sinusoidal waveform. This may be due to the fact that a rectangular waveform with pulse width dependent on frequency delivers more charge per phase at any given frequency and amplitude than the other two waveforms. This preference of rectangular waveform with pulse width dependent on frequency over the two other waveforms was also confirmed by modeling[52-53].

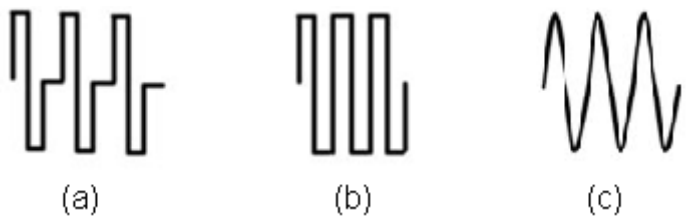

Figure 2: An illustration of the biphasic HFS waveforms. (a) Rectangular with pulse width dependent on frequency. (b) Rectangular with pulse width independent of frequency. (c) Sinusoidal.

HFS with monophasic waveform has been used in nerve conduction block[43, 46, 54-56], but monophasic stimulation is known to be damaging to the tissue and the electrode and therefore are not suitable for chronic applications[57].

It was demonstrated that the interpolar separation distance of a bipolar electrode influences the stimulation amplitudes required to achieve conduction block in both computer simulations and mammalian whole nerve experiements[58]. In computer

simulations, the amplitudes required for conduction block was minimized when the bipolar separation distance was about 2-3 times node lengths for each of the fiber diameter simulated. In experimental results, the optimal bipolar separation distance was 1-2 mm for rat sciatic nerve that has myelinated efferent fibers ranging from 3-14 μm. Bipolar cuff electrodes was shown to be more efficient for nerve block than unipolar electrode via computer modeling, and was also theorized to be more efficient than tripolar cuff electrodes[58].

Furthermore, HFS amplitude required for conduction block was related to the distance between the electrode and the nerve fiber and varied approximately as the square of the perpendicular distance to the axon, according to modeling results for both bipolar and unipolar electrodes[50, 58].

1.3.2 HFS nerve response

Woo and Campbell examined the nerve response to 20 kHz AC (probably sinusoidal) waveform using CAP as well as single fiber recordings[59]. At low amplitudes, axons rhythmically fired at a rate of proximally 100 Hz. As the amplitude increased, the firing frequencies increased up to maximum firing frequency of 400-700 Hz before the axon firing became asynchronous. As the amplitude was further increased to 1-2 V, all firing activity ceased and it was demonstrated that the HFS produced a region of nerve membrane that blocked conduction of action potentials. Bhadra and Kilgore stimulated sciatic nerve in rats with biphasic sinusoidal waveform of 10-30 kHz and 2-10 V and measured the nerve response through the force of gastrocnemius muscle[38]. As shown in

Figure 3, the time response to HFS can be described in three phases. The first phase constitutes an onset response with amplitude similar to or greater than that of a muscle twitch response. The second phase is a period of asynchronous firing featured by slowly decreasing muscle response. The final phase is a steady state of either complete, partial conduction block or no block. The magnitude of the first two phases has been shown to decrease with higher stimulation frequency and amplitude in some[15, 38, 40, 60] but not all studies[21, 41].

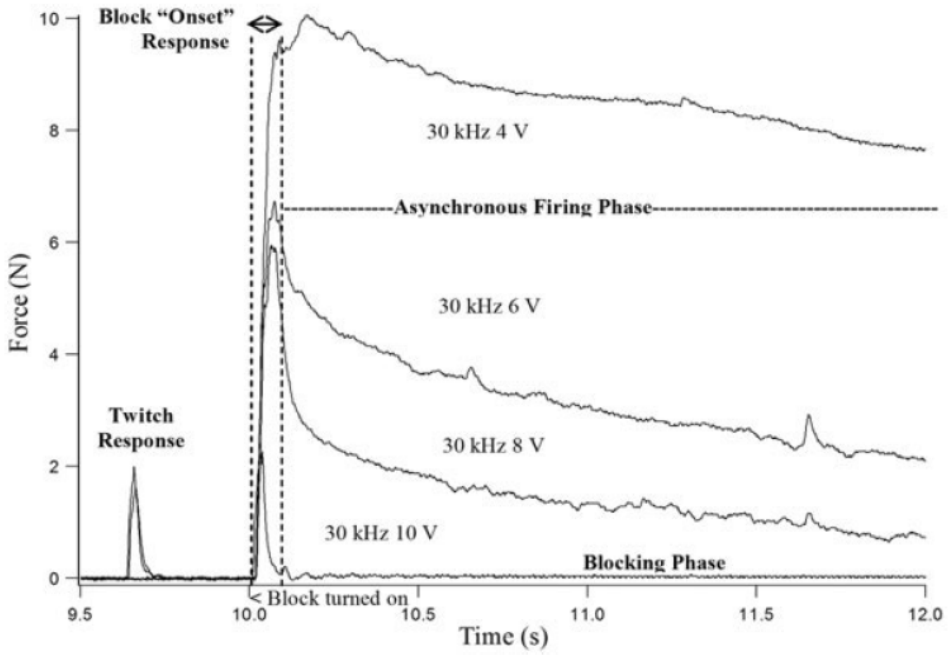

Figure 3: Different phases of the nerve conduction block using biphasic sinusoidal HFS

In some applications partial nerve block, rather than complete nerve block, may be desired in certain patient conditions. HFS allows partial block of a nerve when the amplitude of the blocking waveform is lower than required for complete block. The

transition between partial block and complete block can be done by adjusting the HFS amplitude. However, the transition from partial block to complete block by increasing amplitude is usually accompanied by a second onset response related to this amplitude increase [61].

The onset response and the transient firing may not be desirable for clinical applications due to potential undesirable sensation or stimulation side effect. Various techniques for nerve block induction have been proposed to eliminate or reduce the onset and transient response, including coupling DC with AC waveforms[62] and nerve cooling[63]. In both techniques, after the initial induction technique the nerve block then is maintained by HFS alone. Ramping in amplitude is another proposed technique to minimize the onset response. It has been shown to be successful in eliminating the second onset response when amplitude is increased from a partial block level to a complete block level[61], but not eliminating the initial onset response[64].

1.3.3 Mechanism of action

The mechanism of the HFS nerve conduction block is still under debate. Computer simulations based on the Hodgkin-Huxley (HH) model and the McIntyre, Richardson, and Grill (MRG) model have been used to understand the effects of HFS[19, 21, 44, 50, 52-53, 64-65]. Membrane voltage, ionic currents, and gating potentials near the HFS source were examined. The proposed mechanisms of HFS induced nerve block include net membrane hyperpolarization, deactivation of sodium channels, and the activation of potassium channels.

Recent work by Joseph and Butera suggested that HFS of unmyelinated nerves may have different effects and mechanisms compared to myelinated nerves that are largely studied in the literature [66]. Unlike myelinated nerves where HFS amplitude required for nerve block increased with the stimulation frequencies, HFS amplitude required for blocking an unmyelinated nerve peaked at about 13 kHz and decreased as the frequency increased further. In addition, for an unmyelinated nerve, the recovery time from nerve block after stimulation cessation was shown dependent on the HFS duration. The recovery time of unmyelinated fibers was less than 1 s when the HFS duration was less than 60 s and can be up to 10 s when the HFS duration was greater than 60 s. As a result, the authors proposed that multiple mechanisms may exist for HFS nerve block, especially for unmyelinated nerve fibers.

1.3.4 HFS safety

Although the mechanism of HFS induced nerve conduction block is unclear, HFS may result in changes in intracellular ion concentrations, which may become harmful to the neuron after chronic stimulation. Higher stimulation frequencies have been shown to be more likely to damage nerves[67-68]. On the other side, shorter pulse widths may induce less nerve damage than longer pulse widths[69-70]. HFS of 10 kHz have pulse width maximum of 50 μs, which is one-fourth of the pulse width of 200 μs commonly used in peripheral nerve stimulation. For biphasic HFS, the waveforms are charge-balanced, which is relatively safe compared to unbalanced waveforms[71]. The experimental results of HFS have not been conclusive on the chronic safety. One study in cats showed that biphasic charge-balanced stimulation at a frequency of 1 kHz led to reduction of excitability of the

auditory nerve in cats[72]. A subsequent study in cats showed that biphasic charge balanced stimulation at a frequency of up to 2 kHz was safe for chronic stimulation of the auditory nerve based on physiological and histopathological measurements[73]. In humans, a stimulation frequency of 4.8 kHz was applied to cochlea for up to 3 hours to treat tinnitus and no adverse event such as decrease in hearing was reported[74]. Frequencies as high as 16 kHz have been used in cochlear implant with clinical success[75]. The stimulation amplitudes used in these studies, however, may be lower than what is required for HFS induced nerve block. In summary, the chronic safety of applying biphasic charge-balanced HFS for nerve conduction block is unknown.

1.4 Specific Aims

Nerve conduction block may be used to block undesirable pathological signals and treat diseases that are characterized by pathological afferent and efferent neural activities, such as various pain conditions and muscle spasticity. In spite of research interest by many groups, nerve conduction block by HFS has not been adopted clinically as an available treatment option. Most research has been conducted using cuff electrodes placed encircling a nerve. This demands a complex procedure that may not be accepted by the majority of the patients. While most of the clinical neuromodulation therapies use percutaneous lead electrodes to stimulate the nerves, nerve conduction block experiment using percutaneous lead electrodes has not been reported in the literature.

The overall goal of this work is to characterize peripheral nerve response to HFS delivered through percutaneous lead electrodes in a dog model. First, the feasibility of

biphasic HFS induced nerve block using a percutaneous lead will be evaluated (Aim 1). Specifically, optimal stimulation parameters to achieve nerve block effect and the reversibility of the nerve block will be investigated. The pudendal nerve will be stimulated using a percutaneous lead placed next to the nerve. Motor response of stimulation delivered at the pudendal nerve will be measured by urethral pressure at the external urethral sphincter (EUS) level. Second, pudendal nerve activation threshold at various frequencies will be investigated to further characterize the nerve response to stimulations of high frequencies (Aim 2). Finally, repeatability of the nerve block using percutaneous lead electrodes will be investigated (Aim 3). Repetitive HFS will be delivered for more than 40 minutes and the motor response will be continuously monitored.

2 Materials and Methods

2.1 Animal preparation

All animal care and experimental procedures were performed in accordance with the Guide for the Care and Use of Laboratory Animals published by the National Institutes of Health (National Institutes of Health Publication 85-23, revised 1996) under protocols approved by the Institutional Animal Care and Use Committee at Medtronic Physiological Research Laboratories, Minneapolis, MN. Four (4) intact adult male dogs weighing 25 to 27 kg were anesthetized with propofol (initial dose 4-6 mg/kg intravenously) for induction and anesthesia was maintained by isoflurane (1.0-1.9% expired). An anesthetic monitoring system (AS/3, Datex-Ohmeda) was used to observe body temperature, ECG, blood oxygen saturation, blood pressure, and expired pCO_2. The appropriate depth of anesthesia was maintained by monitoring blood pressure, heart rate, and withdrawal and blink reflexes. Respiration was maintained by a pressure-regulated respirator (7810, Ohmeda) and expired pCO_2 measurements. Body temperature was maintained between 36.6-38.2ºC with a forced warm air (Bair Hugger) temperature management unit. The bilateral pudendal nerves were accessed dorsally between the sciatic notch and the tail on both sides. The pudendal nerve trunks were carefully isolated from the adjacent artery and connective tissue in the ischial rectal fossa. Both nerves were cut to eliminate any effect of the pudendal-to-pudendal spinal reflex on experimental results.

2.2 Experiment Setup and Procedures

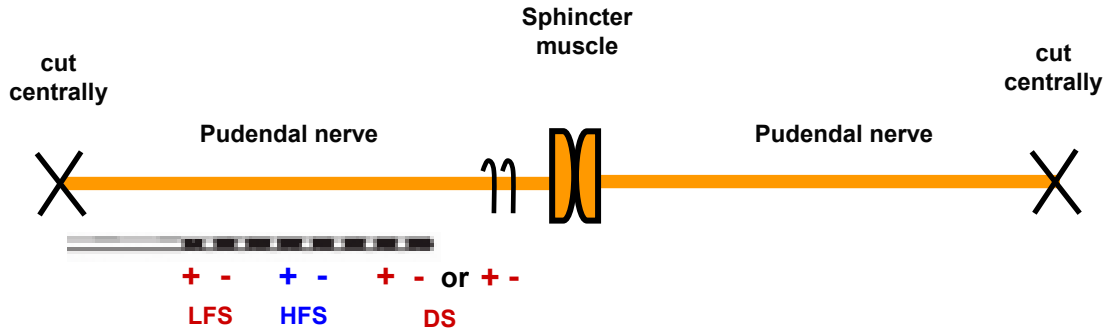

Figure 4: Experimental setup to evoke EUS contraction by LFS and suppress the evoked EUS contractions by HFS of the pudendal nerve.

The experimental setup is illustrated in Figure 4. A percutaneous lead (Medtronic Model 3776) was placed next to the pudendal nerve (usually on the right side). The lead had 8 platinum-iridium electrodes with polyurethane insulation in-between electrodes. Each electrode was 3 mm long, and the separation distance between electrodes was 1.5 mm edge-to-edge. The electrode and lead specifications are listed in Table 1[76]. This lead was designed and FDA approved for Spinal Cord Stimulation (SCS) for pain therapy. It is usually deployed using a minimally invasive percutaneous epidural-access procedure in humans. In this study, a proximal pair of lead electrodes was used to deliver low frequency stimulation (LFS) of 30 Hz to evoke tetanic contraction of the EUS. A middle pair of lead electrodes was used to deliver HFS in the kilohertz range to provide conduction block. In some trials, a distal stimulation (DS) of 1 Hz was delivered by a distal pair of lead electrodes during the HFS to examine the EUS twitch response due to DS during HFS. If the exposed length of the pudendal nerve trunk was not sufficient to allow a distal pair of lead electrodes to be positioned next to the nerve trunk, a pair of

bipolar hook electrodes was used instead to deliver the DS. The muscle and skin layers were reapproximated with suture after saline irrigation.

Table 1: Specifications of percutaneous lead Medtronic Model 3776

Electrode	
Number	8
Length (mm)	3
Individual Surface Area (mm^2)	12
Inter-Electrode Spacing: Edge to Edge (mm)	1.5
Inter-Electrode Spacing: Center to Center (mm)	4.5
Array Length (mm)	35
Lead	
Length (cm)	45
Diameter (mm)	1.3

LFS and DS were generated by custom current-driven stimulators controlled by a computer. HFS was generated by FHC bp Optical Isolator in voltage-driven mode. The pressure signals were amplified and filtered (gain 5000, low pass frequency 10 Hz, sampling rate 250 Hz). All data were collected by a Biopac MP150 system with a 16-bit A/D card. The stimulation waveform for HFS was biphasic charge-balanced square wave with pulse width dependent on frequency (with no pause between cycles), while the waveform for LFS and DS was monophasic square wave with pulse width of 210 μs.
A 7 Fr pressure catheter (9021P5892, Mediwatch) was inserted through the urethra to measure the urethral pressure at the level of the EUS. To facilitate the catheter positioning, a test stimulation train (frequency 1 Hz, pulse width 100 μs, amplitude 0.5 mA) was delivered on the pudendal nerve while the catheter was slowly moved along the urethra. The catheter was positioned such that the urethral pressure port was located at the high pressure zone corresponding to the level of the EUS during the test stimulation.

The procedure includes four parts. First, HFS was delivered alone (*HFS only*) for 20 s at frequencies of 5, 10, 20, 30, and 40 kHz. For each frequency, peak-to peak amplitudes of 5, 10, 15, and 20 V were tested and the order of the trials was randomized. The order of the frequencies tested was also randomized. Second, HFS was delivered in combination with LFS (*HFS+LFS*) to suppress the EUS contraction evoked by the LFS. The same parameters of HFS were tested and the order of the trials was randomized. For each trial, LFS was delivered for 30 s and HFS was delivered for 20 s, starting from 5 s after the LFS initiation and ending at 5 s before the LFS completion. In some trials, DS was delivered during the HFS nerve conduction block to examine EUS twitch response during HFS, and further rule out EUS fatigue. Third, in some animals, HFS of frequencies from 200 Hz to 50 kHz was delivered alone with other stimulations turned off. For each frequency, activation threshold was determined by applying HFS of 20 s duration with amplitudes of 0.1 V peak-to-peak increment until excitation of the EUS was observed from the urethral pressure at the EUS level. Finally, LFS and HFS were delivered for more than 40 minutes to test repeatability of the nerve block effect. LFS was delivered with a repetitive pattern of 2 s on 6 s off. During this time HFS was delivered with a repetitive pattern of 1 minute on, 3 minutes off.

2.3 Data analysis

Block ratio (BR) and block efficiency (BE) were used to quantify the nerve block effect for both *HFS only* and *HFS+LFS* experiments. BR measures the degree of conduction block achieved by HFS. BE measures the efficiency of the nerve block for the entire duration of HFS.

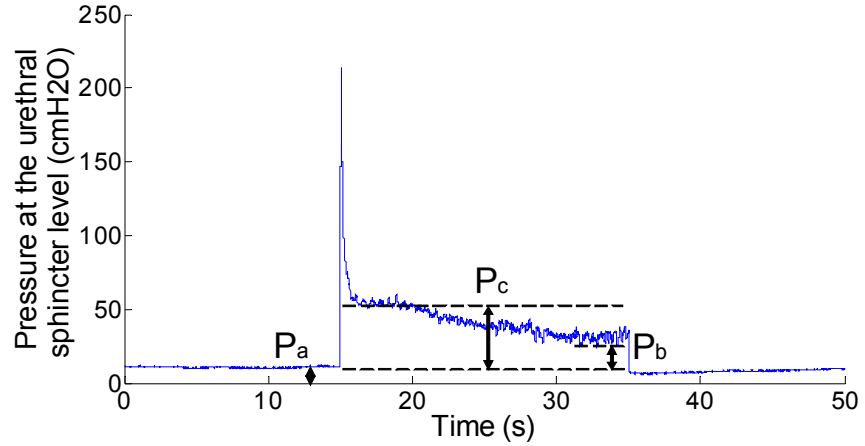

(a)

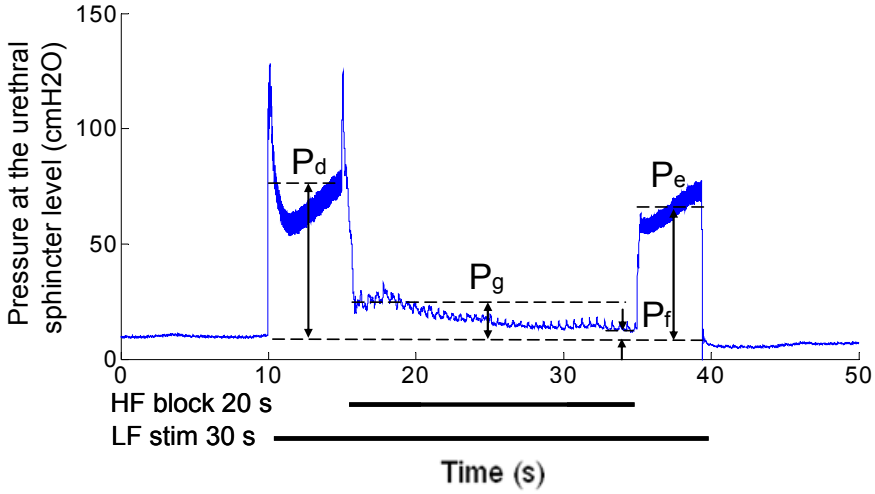

(b)

Figure 5: Measurements of block ratio (BR) and block efficiency (BE) illustrated on typical EUS pressure responses when HFS was delivered alone and when HFS was delivered with LFS. (a) $BR_{HFS} = 1 - P_b/P_a$, $BE_{HFS} = 1 - P_c/P_a$ for *HFS only* experiments. (b) $BR_{HFS+LFS} = (1 - P_f/P_d)\cdot RR$, $BE_{HFS+LFS} = (1 - P_g/P_d)\cdot RR$ for *HFS+LFS* experiments, where $RR = P_e/P_d$.

For *HFS only* experiments, $BR_{HFS} = 1 - P_b/P_a$, where P_a was the baseline pressure at the EUS level and P_b was the difference between the minimum pressure during HFS and the baseline pressure, as shown in Figure 5(a). If the EUS pressure during HFS decreased to

the baseline pressure level ($P_b = 0$), BR_{HFS} was 1 for a complete block. Incomplete or poor nerve block would result in smaller BR_{HF}. For *HFS only* experiments, $BE_{HFS} = 1 - P_c/P_a$, where P_c was the difference between the average pressure during HFS and the baseline pressure at the EUS level (Figure 5(a)). BE_{HFS} was 1 for rapid block effect with no onset and asynchronous response. Poor nerve block efficiency with large onset and prolonged asynchronous firing phase would result in smaller BE_{HFS}. For the purpose of clear data presentation, for HFS parameters where there was lack of activation due to insufficient HFS intensity rather than nerve block, BR_{HFS} and BR_{HFS} were substituted with the lowest values achieved in that animal to represent no block effect.

For *HFS+LFS* experiments, BR and BE took into account a reversibility ratio (RR) to penalize fatigue mechanism versus true nerve block. As shown in Figure 5(b), $RR = P_e/P_d$, where P_d was the average pressure evoked by LFS before HFS minus the baseline pressure, and P_e was the average pressure evoked LFS after HFS minus the baseline pressure. The RR was 1 for full recovery of the LFS evoked EUS response after HFS cessation and 0 for no EUS response after HFS cessation, indicating a fatigue mechanism. As shown in Figure 5(b), $BR_{HFS+LFS} = (1 - P_f/P_d)\cdot RR$, where P_f was the difference between the minimum pressure during HFS and the baseline pressure at the EUS level. Similarly, $BE_{HFS+LFS} = (1 - P_g/P_d)\cdot RR$, where P_g was the difference between the average pressure during HFS and the baseline pressure at the EUS level. Taking into account of RR, for *HFS+LFS* experiments, $BR_{HFS+LFS}$ was 1 for a complete block with full reversibility of the EUS response after HFS, and 0 for no block effect during HFS or

no recovery of the EUS response after HFS, indicating a fatigue mechanism regardless of the EUS pressure suppression effect during HFS.

Digitized data sets were processed using commercial software programs (MATLAB, Math Works, Natick, MA and AcqKnowledge MP150 Manager, BIOPAC Systems, Goleta, CA) to derive the required data variables.

3 Results

3.1 Nerve conduction block and confirmation

For *HFS only* and *HFS+LFS* experiments, complete data sets were collected in three (3) out of 4 dogs. In one dog, stimulation trials were only delivered at certain promising parameters for proof of principle due to time constraint caused by a technical difficulty. Figure 6 shows an example of the pressure responses at the EUS level evoked by HFS alone with parameters of 5, 10, 20, 30, and 40 kHz and 5, 10, 15, and 20 V. The pressure responses generated by HFS plus LFS of the same dog are shown in Figure 7.

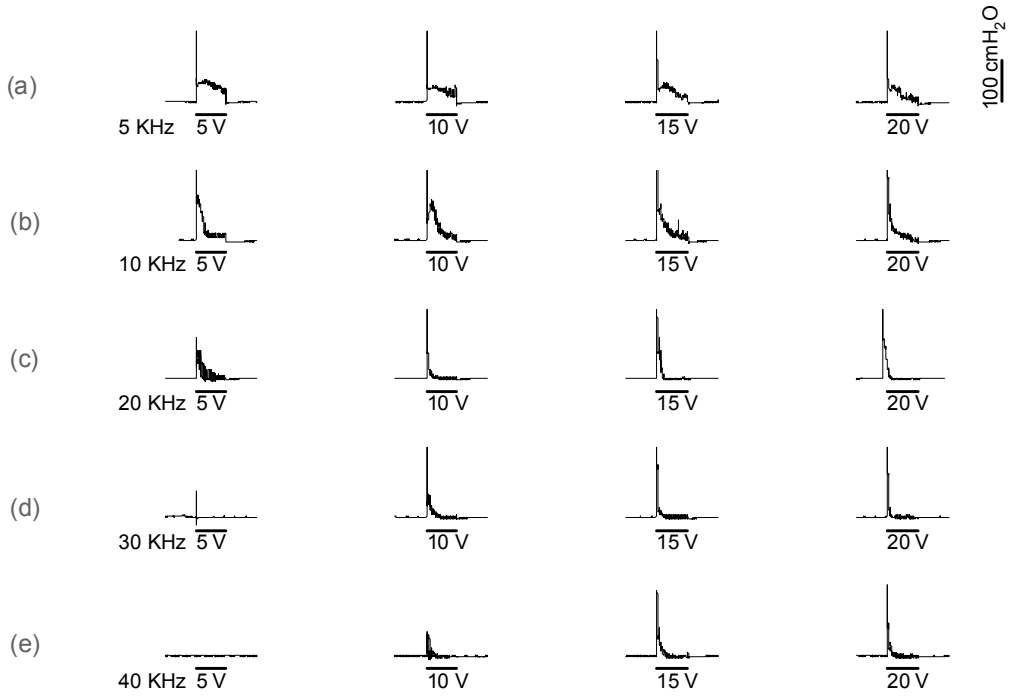

Figure 6: Example of the pressure response at the EUS level in the *HFS only* experiments. HFS of (a) 5 kHz, (b) 10 kHz, (c) 20 kHz, (d) 30 kHz, and (e) 40 kHz of amplitudes 5, 10, 15, and 20 V were delivered. Solid lines underneath the pressure response denote HFS of 20 s duration. Amplitudes tested at each frequency were marked below the solid lines.

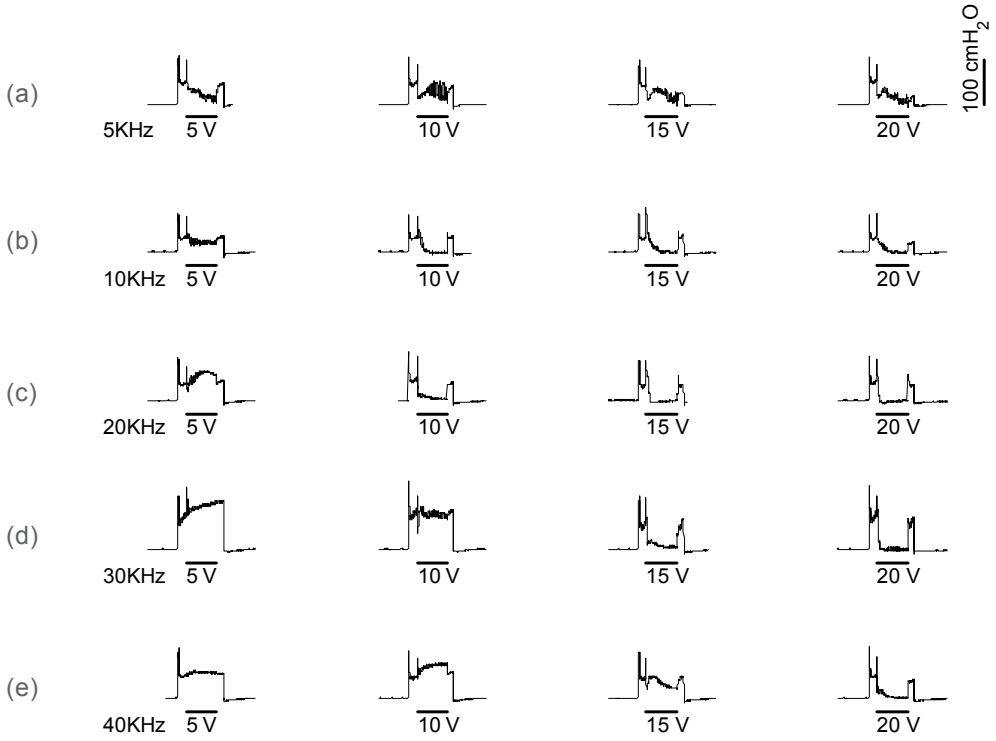

Figure 7: Example of the pressure response at the EUS level in the *HFS+LFS* experiments. HFS of (a) 5 kHz, (b) 10 kHz, (c) 20 kHz, (d) 30 kHz, and (e) 40 kHz of amplitudes 5, 10, 15, and 20 V were delivered. Solid lines underneath the pressure response denote HFS duration of 20 s. LFS of 1.5 mA was delivered for 30 s, with 5 s before HFS, 20 s during HFS, and 5 s after HFS (durations of LFS are not shown).

As shown in Figure 6(a), HFS of 5 kHz induced and maintained EUS contraction that caused elevated urethral pressure throughout the 20 s duration of HFS, although the pressure rapidly decreased during the HFS, especially at higher amplitudes (15 and 20 V). HFS of 5 kHz also produced inadequate suppression of the LFS evoked response (Figure 7(a)). There was poor recovery of the LFS evoked pressure after the cessation of HFS of 5 kHz at higher amplitudes, indicating a fatigue effect. When delivered alone, HFS of 10 kHz elicited less EUS response compared to HFS of 5 kHz. At higher

amplitudes, the EUS response of HFS of 10 kHz decreased close to baseline toward the end of the HFS duration (Figure 6(b)). HFS of 10 kHz was also able to suppress LFS evoked EUS response at higher amplitudes (Figure 7(b)). HFS of 20 and 30 kHz showed good blocking effects at higher but not lower amplitude levels. HFS of 20 and 30 kHz at lower amplitude levels provided poor suppression of the LFS evoked response (Figure 7(c,d)), in spite of lack of EUS contraction response when the HFS was delivered alone (Figure 6(c,d)). This suggests that the lack of EUS contraction with these HFS parameters was due to lack of activation of the EUS, rather than a true nerve block. Similarly, HFS of 40 kHz at lower amplitudes generated zero or minimum EUS response (Figure 6(e)), but demonstrated no suppression or poor suppression of LFS evoked EUS response (Figure 7(e)). This also indicates lack of activation from the HFS versus a true nerve block. HFS of 40 kHz at the highest amplitude of 20 V demonstrated good suppression of LFS evoked EUS response, indicating a nerve block effect (Figure 7(e)).

Figure 8 provides an example of a stimulation trial with DS delivered before, during and after HFS and LFS to confirm a true nerve block by distal nerve activation during HFS. When DS was delivered alone before LFS and HFS started, it elicited a EUS muscle twitch response. The EUS twitch response was replaced with a tetanic EUS contraction when LFS was turned on but HFS remained off. When HFS was turned on in addition to LFS, the tetanic contraction was suppressed but the EUS twitch response elicited by DS was present, indicating a distal activation of the nerve during a true local nerve block versus a fatigue mechanism.

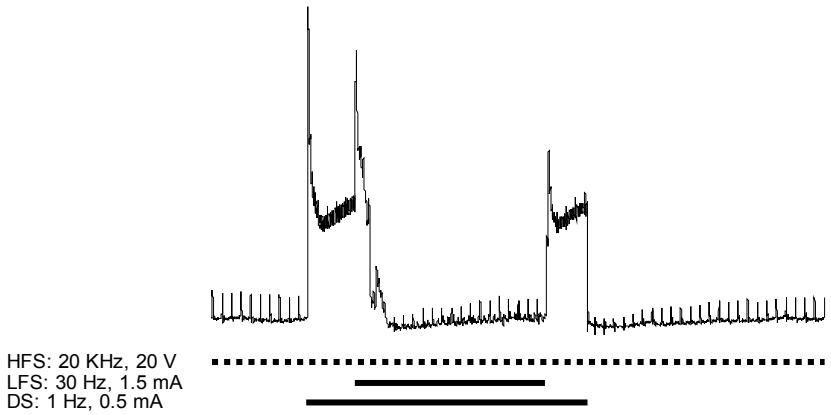

Figure 8: Example of the pressure response at the EUS level in a *HFS+LFS* trial with DS. The solid lines denote the HFS duration (20 s) and LFS duration (30 s). The dotted line denotes DS duration.

3.2 Block ratio and block efficiency

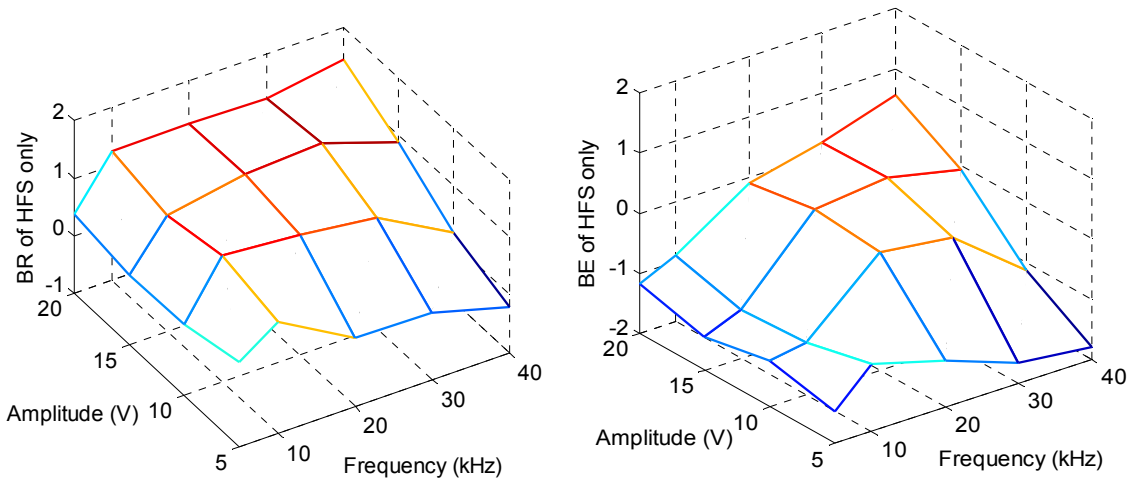

(a) (b)

Figure 9: (a) Block ratio (BR) and (b) block efficiency (BE) of the *HFS only* experiments in 3 dogs.

Figure 9 summarizes the BR and BE of the *HFS only* experiments and Figure 10

summarizes the BR and BE of the *HFS+LFS* experiments. When HFS was delivered alone (Figure 9), BR and BE increased with amplitude, with the exception at the lowest frequency of 5 kHz, where BR and BE remained low over the tested amplitude range due to large EUS contraction response. Similarly, at the lowest amplitude of 5 V, BR and BE of *HFS only* remained low over the tested frequency range. The lack of nerve block at 5 V was in general due to large EUS contraction response with lower frequencies (5 and 10 kHz) and lack of activation but no block with higher frequencies (20, 30, and 40 kHz). At higher amplitudes, BR and BE increased with frequency, but often decreased again at the highest frequency (40 kHz) when amplitudes are not high enough (10 and 15 V).

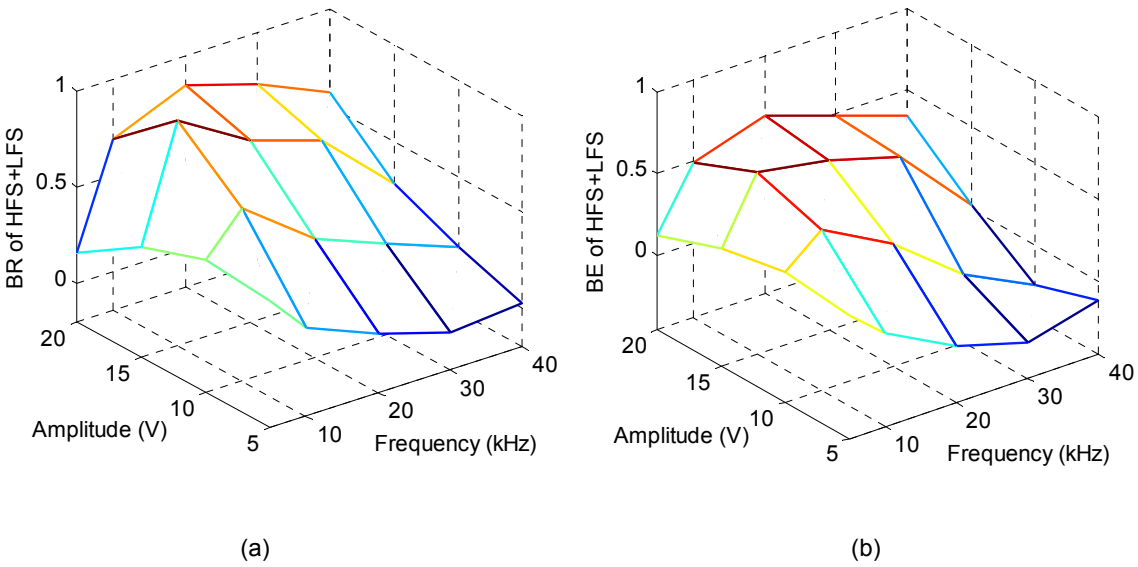

Figure 10: (a) Block ratio (BR) and (b) block efficiency (BE) of the *HFS+LFS* experiments in 3 dogs.

When HFS was delivered together with LFS to suppress the LFS evoked EUS response, BR and BE in general increased with amplitude, with the exception at the lowest

frequency (5 kHz), where BR and BE remained low for all the tested amplitudes due to both insufficient suppression of the EUS response and poor RR (Figure 11). BR and BE of *HFS+LFS* remained low at the lowest amplitude (5 V) over the tested frequency range due to lack of suppression of the LFS response. At higher amplitude levels, BR and BE were higher at mid-frequencies (10, 20, and 30 kHz) compared to those at low frequency of 5 kHz, but decreased again at the highest frequency (40 kHz) due to insufficient suppression of the LFS response.

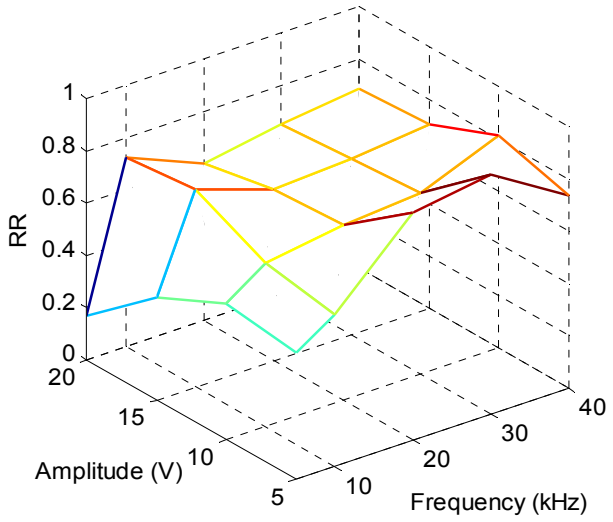

Figure 11: Reversibility ratio (RR) of *HFS+LFS* experiments in 3 dogs.

As shown in Figure 11, reversibility measured by RR was poor for HFS of 5 kHz, especially at higher amplitudes, possibly due to fatigue mechanisms occurred at a frequency level lower than required for nerve block. Note that the RR was higher at higher frequencies, but never reached 1 for complete recovery of the LFS evoked response. This suggests that there may be a certain level of fatigue in some nerve fibers. It is possible that these are nerve fibers that are distant to the percutaneous lead compared

to other fibers in the nerve trunk and might not be in the electric field with enough intensity for nerve block.

The observed latency from the cessation of HFS to a sufficient recovery of the pressure at the EUS level evoked by LFS was in general 300-400 ms. The rise time from initial deployment of LFS to a sufficient rise of Pus was about 100 ms. This suggests that the recovery time from the cessation of HFS to the nerve responding to LFS after HFS was about 200-300 ms. This is within the time frame of fast recovery (<1 s) reported in the literature[77].

3.3 Activation threshold

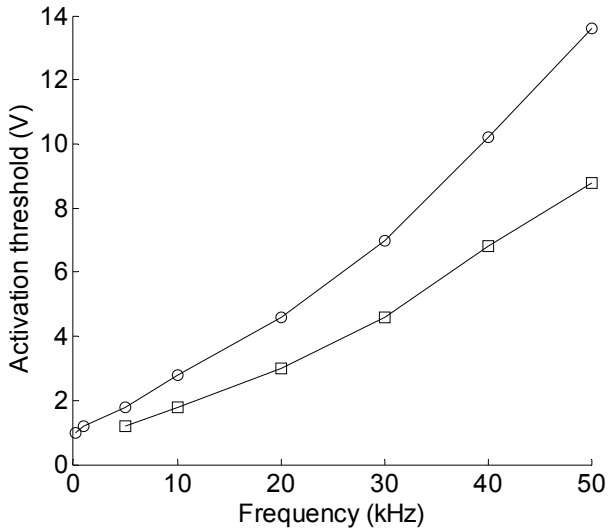

Figure 12: Activation thresholds of HFS measured by pressure response at the EUS level in two dogs. Each curve indicates results from a dog.

To further characterize the nerve response to the biphasic HFS, in two dogs the pudendal

nerve motor activation thresholds measured by the pressure response at the EUS level were tested at various frequencies. As shown in Figure 12, the activation threshold of the biphasic HFS increased with frequency. The activation threshold increased about 8-14 times from 200 Hz to 50 kHz and the increase appeared to be nonlinear. The high activation threshold at high frequencies is consistent with the lack of activation observed with HFS of high frequencies and low amplitudes.

3.4 Repeatability

As shown in Figure 13, pressure response evoked by LFS (2 s on 6 s off) was repeatedly blocked by HFS of 30 kHz and 20 V (1 minute on, 3 minutes) for more than 40 minutes. During the 1 minute duration of each HFS segment, there was a slight gradual reduction of the nerve block effect, indicated by an increased EUS response evoked by repetitive LFS during HFS. This effect was consistent throughout the 40 minutes of stimulation. The block onset and asynchronous firing phase of the HFS segments also prolonged over time during the 40 minutes of repetitive stimulation. This can be observed by comparing the onset and asynchronous firing phase of the first and the last HFS segment, as shown in Figure 13.

The EUS contraction recovered rapidly following each HFS segment of the entire 40 minutes. There was a slight decrease in EUS response amplitude soon after the HFS cessation. The EUS response recovered gradually within the first two minutes of HFS cessation to about 90% of the EUS response of the first pre-HFS segment, but never reached full recovery of the EUS response of the first pre-HFS segment.

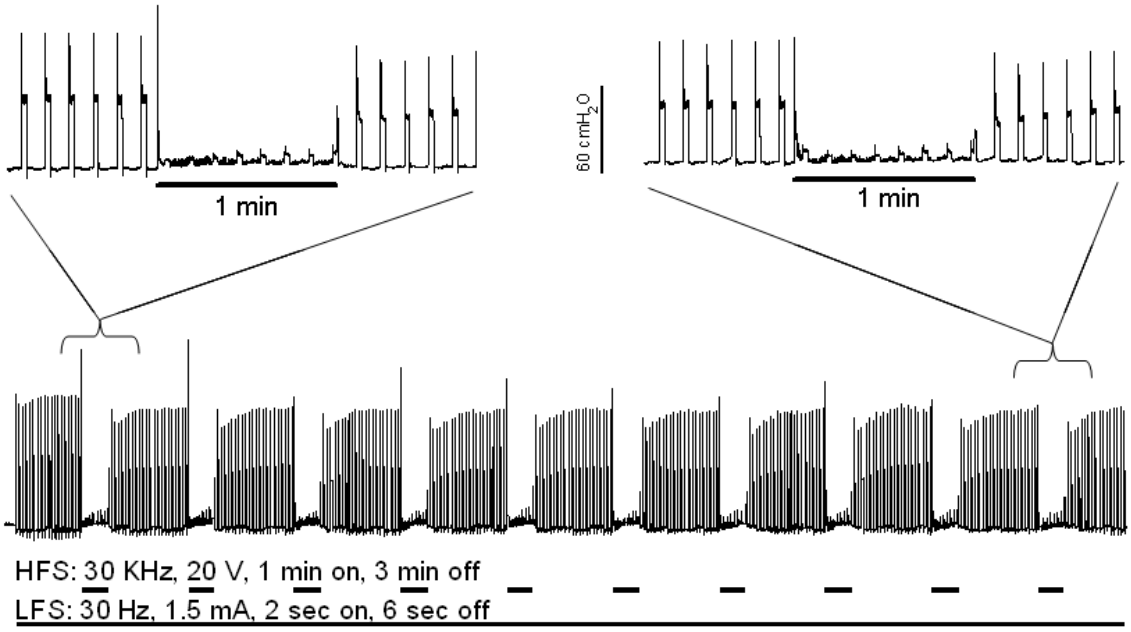

Figure 13: Repeatability of HFS combined with LFS over more than 40 minutes (sec = seconds, min = minutes). The lines underneath the EUS pressure response denote stimulation durations of the HFS and LFS. The first and last HFS segments during the more than 40 minutes of stimulation are enlarged.

Although the repeatability of the LFS response was not a focus of this study, we observed a decrease in LFS evoked EUS response over time in all animals. LFS evoked EUS response at the end of the day of the experiments was 53-75% of the LFS evoked EUS response at the beginning of the day. The decrease in EUS response appeared to be gradual throughout the day. The decrease in EUS response could be due to anesthesia effect, change in the nerve-electrode interface condition, catheter positioning, nerve damage, or muscle fatigue.

4 Discussion

Results from this study demonstrated that the local and reversible nerve block can be achieved with biphasic HFS of high frequencies and amplitudes using a percutaneous lead placed next to the nerve. The optimal frequency and amplitude windows were 10-30 kHz and 15-20 V peak-to-peak within the tested parameter range (5-40 kHz and 5-20 V). It is possible that HFS of 40 kHz requires higher amplitudes to achieve good nerve block effect, but amplitudes higher than 20 V were not tested due to study equipment limitation. Block of EUS contraction by biphasic HFS is attributed to a local conduction block of the pudendal nerve, not fatigue mechanisms. This was confirmed by rapid recovery of EUS contraction evoked by proximal stimulation after HFS, as well as EUS twitch response evoked by distal stimulation during HFS.

Previous reports using cuff electrodes showed that complete nerve block required amplitudes 1-3 V and above for voltage controlled waveforms[38, 41]. In this study, the lowest amplitude that achieved complete suppression of LFS evoked response during HFS was 10 V. This difference in amplitude requirement could be due to a larger distance from the nerve fibers to a lead electrode compared to the distance to a cuff electrode. Modeling results have shown that HFS amplitudes required for conduction block was related to the distance between the electrodes and the nerve fiber and varied approximately as the square of the perpendicular distance to the axon[50, 58]. Assuming that the lead electrodes are placed parallel to the nerve with the lead and the nerve trunk

adjacent to each other, the largest distance between a nerve fiber and a lead electrode is the diameter of the nerve trunk, which is double the largest distance between a nerve fiber and a cuff electrode encircling the nerve. Thus it is reasonable to find that percutaneous lead electrodes require much higher amplitudes for nerve block. The bipolar electrodes configuration with electrode separation distance of 1.5 mm used in this study is comparable to previous studies and within the recommended range for electrode separation for optimal nerve block[58].

Similar to previous findings using cuff electrodes[78], we found that the asynchronous firing phase response could be minimized by higher HFS frequencies and amplitudes, but the initial onset response was not affected by the stimulation parameters. To minimize the asynchronous firing, one approach was to initiate nerve block with the highest frequency and highest amplitude combination available, then decrease the amplitude just enough to maintain the nerve block effect and deliver minimum charge[38]. Based on our findings, this approach may also be applicable to percutaneous leads to reduce asynchronous firing of HFS. However, the onset response of HFS may still cause undesirable sensory and motor responses in clinical applications. Additional technique may be needed to facilitate the nerve block induction, such as DC coupling[62] and nerve cooling[63].

The reversibility ratio never reached 1 for complete recovery even when HFS of high frequencies and amplitudes achieved complete suppression of the LFS evoked response. This suggests that there may be a certain level of fatigue associated with some nerve

fibers (potentially those distant to the percutaneous lead electrodes) and a complete nerve block of all fibers in the nerve trunk is difficult to achieve with a percutaneous lead. In addition, different types of fibers may have different response to HFS, which can be exploited to selectively stimulate or block specific fibers[77]. Nevertheless, a partial block may provide significant clinical benefit. For instance, for the control of muscle spasticity, reducing spastic muscle force may enable the patient to regain enough natural control to accomplish functional activities, whereas a complete block may cause paralysis. For the control of sensory disorders such as pain, reducing the afferent nerve activity from an overactive pathological level to a normal level may be sufficient to benefit the patient but not cause complete loss of sensory input.

For clinical applications of HFS, individual-based parameter titration may be necessary to ensure a desired nerve block effect. Electrophysiological test based on HFS alone may not be sufficient to identify the nerve block effect. For example, in Figure 6(d) HFS of 30 kHz and 10 V showed a typical onset and asynchronous firing response followed by complete relaxation of the EUS. However, when combined with proximal LFS, HFS of these parameters provided minimum suppression of the LFS evoked response, indicating virtually no nerve block effect (Figure 7(d)). In this case the amplitude of 10 V was not high enough to cause nerve block and the electrophysiological response observed with HFS alone was a weak activation response but not nerve block. In another example, HFS of 5 kHz and 20 V and HFS of 10 kHz and 15 V generated similar nerve response in Figure 6(a,b). When combined with LFS, HFS of 10 kHz and 15 V produced nerve block

effect whereas HFS of 5 kHz and 20 V provided insufficient suppression of the LFS evoked response and caused low reversibility after the cessation of the HFS, indicating a fatigue mechanism. On the other hand, titration of HFS parameters based on suppression effect of a simultaneous LFS delivered via separate electrodes may not be desired or possible in a clinical setting. Therefore, it is important to understand the activation threshold of the nerve with high stimulation frequencies and program HFS parameters with sufficient amplitude margin to produce nerve block. Although not a focus of this study, a previous modeling work reported that complete nerve block can be achieved at 2-8 times the activation threshold, depending on the nerve fiber diameter[50]. While it is possible to program the HFS parameters without patient active participation, it is also important to verify the programming based on patient sensory response and motor abilities when the patient is awake and alert after the neuroprosthesis is implanted or during the implant procedure if general anesthesia is not used.

In this study we found that the activation threshold increased nonlinearly as frequency increased. Increase in activation threshold may be due to decrease of charge per phase at higher frequencies. Although there were some controversial results in modeling regarding the relationship between activation threshold and frequency[79], the results from this study is consistent with previous experiments[80-81].

Intermittent biphasic HFS can repeatedly block EUS contraction during a relatively long period (more than 40 minutes). At the end of the 40 minutes of stimulation, a longer onset

and asynchronous firing response was observed compared to that at the beginning of the 40 minutes. EUS contraction recovered rapidly after the HFS was terminated throughout the 40 minutes of stimulation. These findings are consistent with a previous study where repetitive HFS of 1-minute duration was delivered to the pudendal nerve in cats via a cuff electrodes[40]. After repetitive HFS delivered through a nerve cuff, consistent rapid recovery and prolonged onset and asynchronous phases were observed. This previous study also reported that there was no reduction in the block effect during the nerve block phase for each HFS segment and overall after repetitive HFS. However, our results found that for each HFS segment of 1 minute duration, there was a gradual increase of LFS evoked EUS activation response, indicating a decrease of the HFS block effect during 1 minute of continuous HFS. In addition, there was a consistent reduction of EUS response after each HFS segment compared to the EUS response before the first HFS segment (Figure 13). One possible reason for this discrepancy is a fatigue mechanism that requires recovery time of more than 3 minutes in the nerve fibers where nerve block was not achieved using a percutaneous lead. It is worthy to note that although there was reduction of EUS response after the first HFS segment, there was no further reduction of EUS response after the subsequent HFS segments. This suggests the nerve block effect was stable after repetitive HFS for the fibers achieved block.

Long-term safety related to HFS is unknown. The stimulation waveform used in this study was biphasic and charge balanced, which is relatively safe compared to unbalanced waveforms[71]. Key stimulation parameters for safety assessment of electrical stimulation

include charge density, charge per phase, and frequency. The impedance of the lead electrodes measured approximately 500 ohm. Therefore, in an example of HFS of 10 kHz and 20 V peak-to-peak, the stimulation current was about ±20 mA. This gives rise to a charge of 1.0 μC per phase and charge density of 0.083 $\mu C/mm^2$ based on electrode surface area of 12 mm^2. This is within the reported range of safety limits[82-85]. Independent of charge per phase and charge density, HFS may cause tissue damage through overactivation of nerve fibers. Possible mechanisms of damage due to the over excitation of nervous tissue include oxygen or glucose depletion, intracellular or extracellular ion concentration changes, and the excessive release of excitotoxic neurotransmitters such as glutamate. These mechanisms are believed to require stimulation of large regions of nervous tissue. High frequency excitation of any particular fiber or neuron, however, is unlikely to cause nerve damage through overexcitation[68]. Confirmation of neural damage caused by HFS through histological examination is still lacking[86-87]. A study in cats showed that biphasic charge balanced stimulation at a frequency of up to 2 kHz was safe for chronic stimulation[73]. In humans, stimulation frequencies as high as 16 kHz have been used in cochlear implant with clinical success[74-75].

In this study we found that LFS evoked response decreased over time. This effect was also observed in another study using cuff electrodes where force output of the gasrocnemius muscle decreased over time after HFS of the sciatic-tibial nerve in rats[38]. Although this decreased motor response could be attributed to many factors, nerve

damage due to HFS is a possible cause of the effect that has not been sufficiently ruled out. Clinical applications that utilize short durations of HFS, such as control of pelvic floor spasticity during urinary voiding, may have a less stringent requirement for stimulation safety than those that demand a long stimulation time.

There are several limitations of this work. This study has a small sample size and the animals were tested acutely under general anesthesia. EUS pressure response was used as a measure of nerve block effect. This measure only takes into account the response of the larger myelinated fibers but not the smaller lightly myelinated or unmyelinated fibers. Although higher amplitudes may be desired to achieve nerve block at higher frequencies, the amplitudes were tested only up to 20 V peak-to-peak due to equipment limitation.

5 Future work and Conclusion

5.1 Future work

This goal of this research is to develop neuroprostheses using nerve block technology for chronic human use. Clinical use of biphasic HFS for blocking the peripheral nerves will depend on the effectiveness of the technique, demonstration of long-term safety, and tolerability of patient sensations.

5.1.1 Effectiveness of the nerve block using percutaneous lead

Previous reports on HFS using cuff electrodes suggested that stimulation parameters required to block small unmyelinated fibers are different than the parameters required for large myelinated fibers. Through animal experiments and computer modeling, some researchers reported that nerve fibers with smaller diameters require higher amplitudes to achieve nerve block compared to larger fibers[44, 50, 52-53]. Recently other researchers reported HFS amplitude required for blocking an unmyelinated nerve peaked at about 13 kHz and decreased as the frequency increased further. This suggests that HFS of higher frequencies (eg. ≥30 kHz) may produce conduction block of C-fibers at amplitudes lower than needed to block A-fibers[66, 77].

It is possible that optimal HFS parameters for nerve block using a percutaneous lead may also be different for different types of fibers. Nerve recording studies that measure the response of the lightly myelinated and unmyelinated fibers evoked by biphasic HFS using percutaneous lead electrodes are warranted. Sinusoidal waveform may be preferred over the rectangular waveforms for HFS in nerve recording experiments, in order to minimize

sensing artifacts due to stimulation. The ability of HFS to block C-fibers could also be investigated in acute animal models using C-fiber dependent withdrawal reflexes that have been well characterized in the literature[88-90].

Lead design of percutaneous lead electrodes has not been optimized for nerve block. Lead electrode spacing, electrode size and geometry, field steering can be investigated via both simulations and animal experiments. Effects of lead placement, including the distance and the orientation of the lead electrodes relative to a nerve, should also be studied. In general, more work is needed to investigate HFS block using percutaneous lead electrodes or other electrodes that allow for minimally invasive surgical placement to drive patient adoption.

5.1.2 Chronic safety

Although nerve damage due to biphasic HFS has not been evident in acute HFS nerve block studies, chronic safety of HFS for nerve block has not been demonstrated. Chronic HFS experiments are needed to investigate both functional response to chronic HFS and histological measurements after chronic HFS. Safety limits and recommendations on waveform, frequency, charge per phase, charge density, and duty cycle need to be determined. For HFS designed to block one type of fiber, the impact on other types of fibers also need to be considered. For instance, if the HFS parameters required for blocking nociceptive C-fibers are damaging to somatic fibers, it may not be safe to apply HFS neuroprostheses to treat chronic pain.

Preferably, chronic HFS experiments should be conducted with a fully implanted stimulation system. Encapsulation of a chronically implanted lead has been shown to cause stimulation threshold changes over time[91-92]. Similarly, encapsulation may cause incomplete block, longer onset and asynchronous firing duration, or nerve activation and fatigue due to insufficient block amplitude.

5.1.3 Sensory response and other side effects

Sensations elicited by HFS nerve block have not been reported in the literature, yet it is critical to enable clinical applications of HFS. Although it is reasonable to hypothesize that only the onset and asynchronous firing phases of the nerve block response elicit sensations, the relationship between different phases of nerve block response and sensation has not been established. Various techniques have been proposed to reduce onset and asynchronous firing response to HFS[61-63], but the sensations related to the techniques are also unknown. Most animal studies on HFS investigated local nerve response with the animals under general anesthesia. Therefore, system level side effects due to nerve block are also unknown. Animal behavior studies using chronically implanted HFS system should be considered to investigate the sensory response and side effects due to HFS.

5.2 Conclusion

This study demonstrated that it is feasible to achieve local reversible nerve block using percutaneous lead electrodes placed next to a nerve with biphasic HFS waveform. The

optimal frequency and amplitude windows were 10-30 kHz and 15-20 V peak-to-peak within the tested parameter range (5-40 kHz and 5-20 V). It is possible that HFS of 40 kHz and higher requires higher amplitudes beyond the tested range to achieve nerve block. Activation threshold of the nerve evoked by biphasic HFS also increased with frequency. The HFS nerve block was repeatable in more than 40 minutes of repetitive stimulation. Although it may be difficult to block all the nerve fibers in a nerve trunk with a percutaneous lead, partial nerve block can be clinically meaningful to treat many disease conditions.

6 References

1. van Kerrebroeck, P.E.*, et al.* Results of sacral neuromodulation therapy for urinary voiding dysfunction: outcomes of a prospective, worldwide clinical study. *J Urol* **178**, 2029-2034 (2007).
2. Landau, B. & Levy, R.M. Neuromodulation techniques for medically refractory chronic pain. *Annu Rev Med* **44**, 279-287 (1993).
3. Ponce, F.A. & Lozano, A.M. Deep brain stimulation state of the art and novel stimulation targets. *Prog Brain Res* **184**, 311-324 (2010).
4. Abbruzzese, G. The medical management of spasticity. *Eur J Neurol* **9 Suppl 1**, 30-34; discussion 53-61 (2002).
5. Perot, P.L., Jr. & Stein, S.N. Conduction block in peripheral nerve produced by oxygen at high pressure. *Science* **123**, 802-803 (1956).
6. Perot, P.L., Jr. & Stein, S.N. Conduction block in mammalian nerve produced by O2 at high pressure. *Am J Physiol* **197**, 1243-1246 (1959).
7. Franz, D.N. & Iggo, A. Conduction failure in myelinated and non-myelinated axons at low temperatures. *J Physiol* **199**, 319-345 (1968).
8. McMullan, S., Simpson, D.A. & Lumb, B.M. A reliable method for the preferential activation of C- or A-fibre heat nociceptors. *J Neurosci Methods* **138**, 133-139 (2004).
9. Strichartz, G. Molecular mechanisms of nerve block by local anesthetics. *Anesthesiology* **45**, 421-441 (1976).
10. Ashburn, M.A. & Staats, P.S. Management of chronic pain. *Lancet* **353**, 1865-1869 (1999).
11. Guven, M., Ozgunen, K. & Gunay, I. Conduction blocks of lidocaine on crushed rat sciatic nerve: an in-vitro study. *Int J Neurosci* **115**, 725-734 (2005).
12. Guven, M.*, et al.* The actions of lamotrigine and levetiracetam on the conduction properties of isolated rat sciatic nerve. *Eur J Pharmacol* **553**, 129-134 (2006).
13. Martinov, V.N. & Nja, A. A microcapsule technique for long-term conduction block of the sciatic nerve by tetrodotoxin. *J Neurosci Methods* **141**, 199-205 (2005).
14. Cattell, M. & Gerard, R.W. The "inhibitory" effect of high-frequency stimulation and the excitation state of nerve. *J Physiol* **83**, 407-415 (1935).
15. Rosenblueth, A.a.R., J. The blocking and deblocking effects of alternating currents on nerve. *American Journal of Physiology* **125**, 251-264 (1939).
16. Jensen, A.L. & Durand, D.M. High frequency stimulation can block axonal conduction. *Exp Neurol* **220**, 57-70 (2009).
17. Bellinger, S.C., Miyazawa, G. & Steinmetz, P.N. Submyelin potassium accumulation may functionally block subsets of local axons during deep brain stimulation: a modeling study. *J Neural Eng* **5**, 263-274 (2008).
18. Liu, H., Roppolo, J.R., de Groat, W.C. & Tai, C. Modulation of axonal excitability by high-frequency biphasic electrical current. *IEEE Trans Biomed Eng* **56**, 2167-2176 (2009).

19. Zhang, X., Roppolo, J.R., de Groat, W.C. & Tai, C. Mechanism of nerve conduction block induced by high-frequency biphasic electrical currents. *IEEE Trans Biomed Eng* **53**, 2445-2454 (2006).
20. Tai, C., Wang, J., Roppolo, J.R. & de Groat, W.C. Relationship between temperature and stimulation frequency in conduction block of amphibian myelinated axon. *J Comput Neurosci* **26**, 331-338 (2009).
21. Kilgore, K.L. & Bhadra, N. Nerve conduction block utilising high-frequency alternating current. *Med Biol Eng Comput* **42**, 394-406 (2004).
22. Petruska, J.C., Hubscher, C.H. & Johnson, R.D. Anodally focused polarization of peripheral nerve allows discrimination of myelinated and unmyelinated fiber input to brainstem nuclei. *Exp Brain Res* **121**, 379-390 (1998).
23. Bhadra, N. & Kilgore, K.L. Direct current electrical conduction block of peripheral nerve. *IEEE Trans Neural Syst Rehabil Eng* **12**, 313-324 (2004).
24. Whitwam, J.G. & Kidd, C. The use of direct current to cause selective block of large fibres in peripheral nerves. *Br J Anaesth* **47**, 1123-1133 (1975).
25. van den Honert, C. & Mortimer, J.T. A technique for collision block of peripheral nerve: frequency dependence. *IEEE Trans Biomed Eng* **28**, 379-382 (1981).
26. van den Honert, C. & Mortimer, J.T. A technique for collision block of peripheral nerve: single stimulus analysis. *IEEE Trans Biomed Eng* **28**, 373-378 (1981).
27. Bikson, M.*, et al.* Suppression of epileptiform activity by high frequency sinusoidal fields in rat hippocampal slices. *J Physiol* **531**, 181-191 (2001).
28. Jensen, A.L. & Durand, D.M. Suppression of axonal conduction by sinusoidal stimulation in rat hippocampus in vitro. *J Neural Eng* **4**, 1-16 (2007).
29. Anderson, M.E., Postupna, N. & Ruffo, M. Effects of high-frequency stimulation in the internal globus pallidus on the activity of thalamic neurons in the awake monkey. *J Neurophysiol* **89**, 1150-1160 (2003).
30. Hashimoto, T., Elder, C.M., Okun, M.S., Patrick, S.K. & Vitek, J.L. Stimulation of the subthalamic nucleus changes the firing pattern of pallidal neurons. *J Neurosci* **23**, 1916-1923 (2003).
31. Jech, R.*, et al.* Functional magnetic resonance imaging during deep brain stimulation: a pilot study in four patients with Parkinson's disease. *Mov Disord* **16**, 1126-1132 (2001).
32. McIntyre, C.C., Grill, W.M., Sherman, D.L. & Thakor, N.V. Cellular effects of deep brain stimulation: model-based analysis of activation and inhibition. *J Neurophysiol* **91**, 1457-1469 (2004).
33. Windels, F.*, et al.* Effects of high frequency stimulation of subthalamic nucleus on extracellular glutamate and GABA in substantia nigra and globus pallidus in the normal rat. *Eur J Neurosci* **12**, 4141-4146 (2000).
34. Foffani, G. & Priori, A. Deep brain stimulation in Parkinson's disease can mimic the 300 Hz subthalamic rhythm. *Brain* **129**, e59; author reply e60 (2006).
35. Garcia, L., D'Alessandro, G., Bioulac, B. & Hammond, C. High-frequency stimulation in Parkinson's disease: more or less? *Trends Neurosci* **28**, 209-216 (2005).
36. Grill, W.M., Snyder, A.N. & Miocinovic, S. Deep brain stimulation creates an informational lesion of the stimulated nucleus. *Neuroreport* **15**, 1137-1140 (2004).

37. Vitek, J.L. Mechanisms of deep brain stimulation: excitation or inhibition. *Mov Disord* **17 Suppl 3**, S69-72 (2002).
38. Bhadra, N. & Kilgore, K.L. High-frequency electrical conduction block of mammalian peripheral motor nerve. *Muscle Nerve* **32**, 782-790 (2005).
39. Tai, C., Roppolo, J.R. & de Groat, W.C. Block of external urethral sphincter contraction by high frequency electrical stimulation of pudendal nerve. *J Urol* **172**, 2069-2072 (2004).
40. Tai, C., Roppolo, J.R. & de Groat, W.C. Response of external urethral sphincter to high frequency biphasic electrical stimulation of pudendal nerve. *J Urol* **174**, 782-786 (2005).
41. Bhadra, N., Kilgore, K. & Gustafson, K.J. High frequency electrical conduction block of the pudendal nerve. *J Neural Eng* **3**, 180-187 (2006).
42. Tanner, J.A. Reversible blocking of nerve conduction by alternating-current excitation. *Nature* **195**, 712-713 (1962).
43. Ishigooka, M., Hashimoto, T., Sasagawa, I., Izumiya, K. & Nakada, T. Modulation of the urethral pressure by high-frequency block stimulus in dogs. *Eur Urol* **25**, 334-337 (1994).
44. Williamson, R.P. & Andrews, B.J. Localized electrical nerve blocking. *IEEE Trans Biomed Eng* **52**, 362-370 (2005).
45. Forbes, A.a.R., L. Quantitative studies of the nerve impulse IV. Fatigue in peripheral nerve. *Am. J. Physiol.* **90**, 119-145 (1929).
46. Solomonow, M., Eldred, E., Lyman, J. & Foster, J. Control of muscle contractile force through indirect high-frequency stimulation. *Am J Phys Med* **62**, 71-82 (1983).
47. Abdel-Gawad, M., Boyer, S., Sawan, M. & Elhilali, M.M. Reduction of bladder outlet resistance by selective stimulation of the ventral sacral root using high frequency blockade: a chronic study in spinal cord transected dogs. *J Urol* **166**, 728-733 (2001).
48. Shaker, H.S.*, et al.* Reduction of bladder outlet resistance by selective sacral root stimulation using high-frequency blockade in dogs: an acute study. *J Urol* **160**, 901-907 (1998).
49. Bowman, B.R. & McNeal, D.R. Response of single alpha motoneurons to high-frequency pulse trains. Firing behavior and conduction block phenomenon. *Appl Neurophysiol* **49**, 121-138 (1986).
50. Bhadra, N., Lahowetz, E.A., Foldes, S.T. & Kilgore, K.L. Simulation of high-frequency sinusoidal electrical block of mammalian myelinated axons. *J Comput Neurosci* **22**, 313-326 (2007).
51. Ackermann, D.M., Jr., Foldes, E.L., Bhadra, N. & Kilgore, K.L. Conduction block of peripheral nerve using high-frequency alternating currents delivered through an intrafascicular electrode. *Muscle Nerve* **41**, 117-119 (2010).
52. Tai, C., de Groat, W.C. & Roppolo, J.R. Simulation analysis of conduction block in unmyelinated axons induced by high-frequency biphasic electrical currents. *IEEE Trans Biomed Eng* **52**, 1323-1332 (2005).
53. Tai, C., de Groat, W.C. & Roppolo, J.R. Simulation of nerve block by high-frequency sinusoidal electrical current based on the Hodgkin-Huxley model. *IEEE Trans Neural Syst Rehabil Eng* **13**, 415-422 (2005).

54. Solomonow, M. External control of the neuromuscular system. *IEEE Trans Biomed Eng* **31**, 752-763 (1984).
55. Zhou, B.H., Baratta, R. & Solomonow, M. Manipulation of muscle force with various firing rate and recruitment control strategies. *IEEE Trans Biomed Eng* **34**, 128-139 (1987).
56. Baratta, R., Ichie, M., Hwang, S.K. & Solomonow, M. Orderly stimulation of skeletal muscle motor units with tripolar nerve cuff electrode. *IEEE Trans Biomed Eng* **36**, 836-843 (1989).
57. Mortimer, J.T. Motor prostheses. in *Handbook of physiology, section 1: the nervous system - vol. II motor control, Part 1* (ed. J.M. Brookhart, Mountcastle, V. B., Brooks, V. B., and Geiger, S.R.) 155-187 (Ameri. Physiol. Soc., Bethesda, USA, 1981).
58. Ackermann, D.M., Jr., Foldes, E.L., Bhadra, N. & Kilgore, K.L. Effect of bipolar cuff electrode design on block thresholds in high-frequency electrical neural conduction block. *IEEE Trans Neural Syst Rehabil Eng* **17**, 469-477 (2009).
59. Woo, M.Y. & Campbell, B. Asynchronous Firing and Block of Peripheral Nerve Conduction by 20 Kc Alternating Current. *Bull Los Angel Neuro Soc* **29**, 87-94 (1964).
60. Gaunt, R.A. & Prochazka, A. Transcutaneously coupled, high-frequency electrical stimulation of the pudendal nerve blocks external urethral sphincter contractions. *Neurorehabil Neural Repair* **23**, 615-626 (2009).
61. Bhadra, N., Foldes, E.L., Ackermann, D. & Kilgore, K.L. Reduction of the onset response in high frequency nerve block with amplitude ramps from non-zero amplitudes. *Conf Proc IEEE Eng Med Biol Soc* **2009**, 650-653 (2009).
62. Kilgore, K.L., Foldes, E.A., Ackermann, D.M. & Bhadra, N. Combined direct current and high frequency nerve block for elimination of the onset response. *Conf Proc IEEE Eng Med Biol Soc* **2009**, 197-199 (2009).
63. Ackermann, D.M., Foldes, E.L., Bhadra, N. & Kilgore, K.L. Nerve conduction block using combined thermoelectric cooling and high frequency electrical stimulation. *J Neurosci Methods* **193**, 72-76 (2010).
64. Miles, J.D., Kilgore, K.L., Bhadra, N. & Lahowetz, E.A. Effects of ramped amplitude waveforms on the onset response of high-frequency mammalian nerve block. *J Neural Eng* **4**, 390-398 (2007).
65. Wang, J., Shen, B., Roppolo, J.R., de Groat, W.C. & Tai, C. Influence of frequency and temperature on the mechanisms of nerve conduction block induced by high-frequency biphasic electrical current. *J Comput Neurosci* **24**, 195-206 (2008).
66. Joseph, L. & Butera, R.J. Unmyelinated Aplysia nerves exhibit a nonmonotonic blocking response to high-frequency stimulation. *IEEE Trans Neural Syst Rehabil Eng* **17**, 537-544 (2009).
67. Agnew, W.F., McCreery, D.B., Yuen, T.G. & Bullara, L.A. Histologic and physiologic evaluation of electrically stimulated peripheral nerve: considerations for the selection of parameters. *Ann Biomed Eng* **17**, 39-60 (1989).
68. McCreery, D.B., Agnew, W.F., Yuen, T.G. & Bullara, L.A. Relationship between stimulus amplitude, stimulus frequency and neural damage during electrical stimulation of sciatic nerve of cat. *Med Biol Eng Comput* **33**, 426-429 (1995).

69. McCreery, D.B., Agnew, W.F., Yuen, T.G. & Bullara, L. Charge density and charge per phase as cofactors in neural injury induced by electrical stimulation. *IEEE Trans Biomed Eng* **37**, 996-1001 (1990).
70. McCreery, D.B., Agnew, W.F., Yuen, T.G. & Bullara, L.A. Damage in peripheral nerve from continuous electrical stimulation: comparison of two stimulus waveforms. *Med Biol Eng Comput* **30**, 109-114 (1992).
71. Agnew, W.F.a.M., D. B. *Neural Prostheses: Fundamental Studies* (Prentice Hall, Englewood Cliffs, New Jersey, 1990).
72. Tykocinski, M., Shepherd, R.K. & Clark, G.M. Reduction in excitability of the auditory nerve following electrical stimulation at high stimulus rates. *Hear Res* **88**, 124-142 (1995).
73. Xu, J., Shepherd, R.K., Millard, R.E. & Clark, G.M. Chronic electrical stimulation of the auditory nerve at high stimulus rates: a physiological and histopathological study. *Hear Res* **105**, 1-29 (1997).
74. Rubinstein, J.T., Tyler, R.S., Johnson, A. & Brown, C.J. Electrical suppression of tinnitus with high-rate pulse trains. *Otol Neurotol* **24**, 478-485 (2003).
75. Waltzman, S.B.a.R., J. T. Jr. *Cochlear Implants* (Thieme Medical Publishers, New York, NY, 2006).
76. Medtronic, I. Medtronic 1x8 SC 3776 3876, 1x8 3777 3877, 1x8 COMPACT 3778 3878 low impedance lead kit mannual. (2008).
77. Joseph, L. Conduction block in perpheral nerves: effect of high frequency stimulation on different fiber types. in *Ph.D. thesis, Department of Biomedical Engineering* 121 (Georgia Institute of Technology, Atlanta, GA, 2010).
78. Foldes, E.L., Ackermann, D., Bhadra, N. & Kilgore, K.L. Counted cycles method to quantify the onset response in high-frequency peripheral nerve block. *Conf Proc IEEE Eng Med Biol Soc* **2009**, 614-617 (2009).
79. Katz, B. Nerve excitation by high-frequency alternating current. *J Physiol* **96**, 202-224 (1939).
80. Tasaki, I. & Sato, M. On the relation of the strength-frequency curve in excitation by alternating current to the strength-duration and latent addition curves of the nerve fiber. *J Gen Physiol* **34**, 373-388 (1951).
81. Guttman, R. & Hachmeister, L. Effect of calcium, temperature, and polarizing currents upon alternating current excitation of space-clamped squid axons. *J Gen Physiol* **58**, 304-321 (1971).
82. Brummer, S.B. & Turner, M.J. Electrical stimulation with Pt electrodes: II-estimation of maximum surface redox (theoretical non-gassing) limits. *IEEE Trans Biomed Eng* **24**, 440-443 (1977).
83. Brummer, S.B. & Turner, M.J. Electrical stimulation with Pt electrodes: I-a method for determination of "real" electrode areas. *IEEE Trans Biomed Eng* **24**, 436-439 (1977).
84. Brummer, S.B., McHardy, J. & Turner, M.J. Electrical stimulation with Pt electrodes: Trace analysis for dissolved platinum and other dissolved electrochemical products. *Brain Behav Evol* **14**, 10-22 (1977).

85. Merrill, D.R., Bikson, M. & Jefferys, J.G. Electrical stimulation of excitable tissue: design of efficacious and safe protocols. *J Neurosci Methods* **141**, 171-198 (2005).
86. Agnew, W.F., McCreery, D.B., Yuen, T.G. & Bullara, L.A. Evolution and resolution of stimulation-induced axonal injury in peripheral nerve. *Muscle Nerve* **22**, 1393-1402 (1999).
87. McCreery, D.B., Yuen, T.G. & Bullara, L.A. Chronic microstimulation in the feline ventral cochlear nucleus: physiologic and histologic effects. *Hear Res* **149**, 223-238 (2000).
88. Clarke, R.W., Ford, T.W. & Taylor, J.S. Reflex actions of selective stimulation of sural nerve C fibres in the rabbit. *Q J Exp Physiol* **74**, 681-690 (1989).
89. Iwamoto, G.A., Ryu, H. & Wagman, I.H. Contribution of unmyelinated afferents from the sural nerve to spinal reflex activity. *Exp Neurol* **62**, 260-267 (1978).
90. Wall, P.D. & Woolf, C.J. Muscle but not cutaneous C-afferent input produces prolonged increases in the excitability of the flexion reflex in the rat. *J Physiol* **356**, 443-458 (1984).
91. Grill, W.M. & Mortimer, J.T. Electrical properties of implant encapsulation tissue. *Ann Biomed Eng* **22**, 23-33 (1994).
92. Grill, W.M. & Mortimer, J.T. Stability of the input-output properties of chronically implanted multiple contact nerve cuff stimulating electrodes. *IEEE Trans Rehabil Eng* **6**, 364-373 (1998).